Ion Coordination in the Amphotericin B Channel

Vitaly Khutorsky
Department of Chemistry, Ben Gurion University of the Negev, Beer Sheva 84 105, Israel

ABSTRACT The antifungal polyene antibiotic amphotericin B forms channels in lipid membranes that are permeable to ions, water, and nonelectrolytes. Anion, cation, and ion pair coordination in the water-filled pore of the "barrel" unit of the channels was studied by molecular dynamics simulations. Unlike the case of the gramicidin A channel, the water molecules do not create a single-file configuration in the pore, and some cross sections of the channel contain three or four water molecules. Both the anion and cation are strongly bound to ligand groups and water molecules located in the channel. The coordination number of the ions is about six. The chloride has two binding sites in the pore. The binding with water is dominant; more than four water molecules are localized in the anion coordination sphere. Three motifs of the ion coordination were monitored. The dominant motif occurs when the anion is bound to one ligand group. The ion is bound to two or three ligand groups in the less favorable configurations. The strong affinity of cations to the channel is determined by the negatively charged ligand oxygens, whose electrostatic field dominates over the field of the hydrogens. The ligand contribution to the coordination number of the sodium ion is noticeably higher than in the case of the anion. As in the case of the anion, there are three motifs of the cation coordination. The favorable one occurs when the cation is bound to two ligand oxygens. In the less favorable cases, the cation is bound to three or four oxygens. In the contact ion pair, the cation and anion are bound to two ligand oxygens and one ligand hydrogen, respectively. There exist intermediate solvent-shared states of the ion pair. The average distances between ions in these states are twice as large as that of the contact ion pair. The stability of the solvent-shared state is defined by the water molecule oriented along the electrostatic field of both ions.

INTRODUCTION

The polyene antibiotics amphotericin B and nystatin are important drugs that are widely used to treat serious systemic fungal infections (see reviews of Brajtburg et al., 1990, and Gallis et al., 1990). The molecules feature a lactone ring containing conjugated double bonds, a chain of hydrophilic groups, and two ionizable groups—a carboxyl and a mycosamine (Fig. 1). In the nystatin molecule one double bond is hydrogenated. The antibiotics form channels in lipid membranes that are permeable to ions, water, and nonelectrolytes. Single ionic channels formed by amphotericin B and nystatin were observed and examined (Ermishkin et al., 1976, 1977). The channels have conducting and nonconducting states, with frequent transitions between them. One can induce a rise in conductance with amphotericin B or nystatin on one or both sides of the planar bilayer membranes (see references in the review of Bolard, 1986). The permeability coefficients decrease monotonically with increasing molecular size of the nonelectrolytes in the order water > urea > ethylene glycol > glycerol and are very small for molecules that are of the size of glucose. The molecules of larger size are essentially impermeant (De Kruijff et al., 1974; Cohen, 1986). When the antibiotic is added to both sides, the electrical conductance is much larger and the permeability of univalent anions is larger than that of the cations. Under certain conditions the selectivity is very high (Borisova et al., 1986). When the antibiotic is added to only one side, it is selective to univalent cations.

The damaging action of the antibiotics to cells originates from their binding to sterols incorporated in cellular membranes. More effective binding to ergosterol and ergosterol-containing membranes than to cholesterol and cholesterol-containing membranes was demonstrated by spectrophotometry (Gruda et al., 1980; Vertut-Croquin et al., 1983). Herve et al. (1989) concluded that the alkyl side chain of ergosterol with the double bond located in the middle of the chain was responsible for the greater sensitivity to the polyene antibiotics of ergosterol-containing membranes. The cholesterol alkyl side chain is more flexible. The flat shape of the ergosterol molecule may facilitate intermolecular contacts with the flat polyene antibiotics. It can be expected that the nonspecific binding to sterol of nystatin with a more flexible chain composed of two and four double bonds is weaker than the binding of amphotericin B with a chain of seven conjugated double bonds. Consistent with this reasoning, nystatin differs greatly from amphotericin B in relative potency toward fungal and mammalian cells (see review of Brajtburg et al., 1990).

Amphotericin B and nystatin form two types of channels that are structurally very similar but differ in length by a factor of 2. It is assumed that the channels are formed by one or two "barrels" consisting of antibiotics and incorporated sterol molecules, with the long axes oriented perpendicularly to the membrane surface (Andreoli, 1973; De Kruijff and Demel, 1974; Finkelstein and Holz, 1973). The hydrophilic, charged, and hydrophobic sides of the antibi

Received for publication 18 August 1995 and in final form 9 September 1996.

Address reprint requests to Dr. Vitaly Khutorsky, Department of Chemistry, Ben-Gurion University of the Negev, P.O.B. 653, Beer-Sheva 84 105, Israel. Tel.: 972-7-6494945; Fax: 972-7-6472943; E-mail: vitalik@bgumail.bgu.ac.il.

0006-3495/96/12/2984/12 $2.00

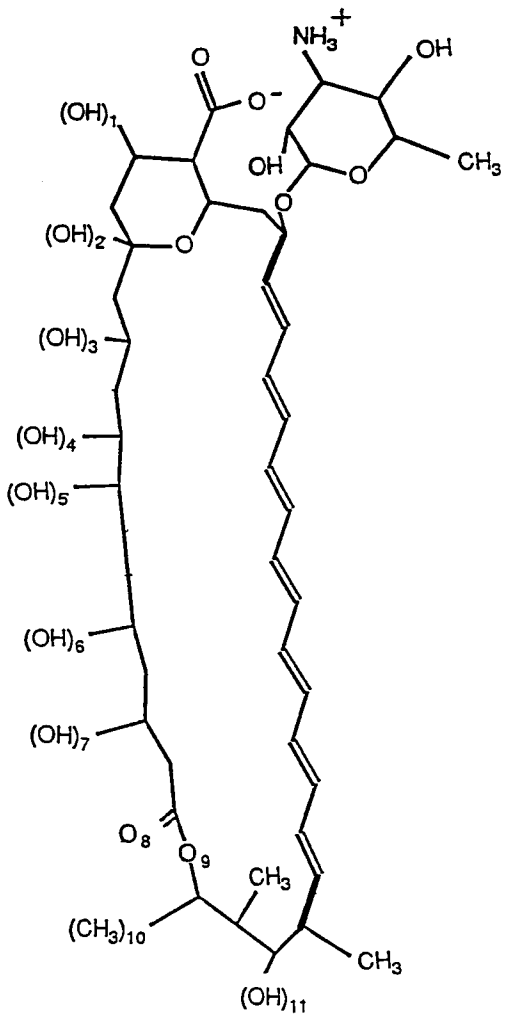

FIGURE 1 Structure of amphotericin B. The ligand groups are enumerated. The conjugated double bond system is omitted in MD simulations. The fixed edge bonds of the remaining molecule are represented by thick lines.

otic molecules are turned toward the water pore, water, and lipid phases, respectively. Later it was shown that the conductance and selectivity of the channels are not influenced by changes in the charged groups (Kasumov et al., 1979). These properties strongly depend on the structure of the polar chain of the lactone ring that additionally supports the proposed model. Different channel molarities have been reported (Cass et al., 1970; De Kruijff and Demel, 1974; Van Hoogevest and De Kruijff, 1978; Bolina-Marin et al., 1991), with the number of asymmetrical units ranging from 4 to 12. In spite of this variability, the selectivity of the channels does not seem to change. Eight asymmetrical units per barrel yields a 8-Å-diameter pore that may exclude molecules larger than glucose. The two types of channels show the same relative permeability to urea and glycerol, indicating that the channel radii are the same. The one-sided action is attributable to channels having essentially the same structure as those formed by the two-sided action, except that only one "barrel" (half-pore) spanned the bilayer to form a functional channel (Marty and Finkelstein, 1975). The two-sided channels are formed by two barrels bound end to end in the membranes (Van Hoogevest and De Kruijff, 1978; Marty and Finkelstein, 1975; Bolard et al., 1991). It may appear surprising that both channels can be accommodated by membranes. The length of the half-pore is about 25 Å. The maximum bilayer thickness should be beyond which the antibiotics are ineffective from one side, because the channel is not long enough to span the bilayer and the possibility of the "flip-flop" has been ruled out experimentally. This assumption was tested on membranes of increasing thickness (Van Hoogevest and De Kruijff, 1978; Kleinberg and Finkelstein, 1984). The thicknesses of the hydrophobic interior of membranes increase monotonically with the number of carbons in acyl chains (Benz et al., 1975; Kleinberg and Finkelstein, 1984). The length of the hydrophobic portion of the antibiotics is close to the experimentally measured thickness of the hydrophobic interior of membranes, with the number of carbon atoms in acyl chains ranging from 14 to 18 (Kleinberg and Finkelstein, 1984). Whereas these membranes were very sensitive to the one-sided action, the membranes with longer chains were totally refractory (Van Hoogevest and De Kruijff, 1978; Kleinberg and Finkelstein, 1984). All membranes were sensitive to the two-sided action. It was argued that sufficient flexibility exists in the unperturbed bilayer to accommodate the double-length channel (Kleinberg and Finkelstein, 1984). In this state the acyl chains of the lipid are compressed to about 60% of their fully stretched length and can apparently extend to accommodate the double-length channels. The double-length channel lifetime is considerably longer than the lifetime of channels formed by one-sided action, probably because the hydrophobic end of the latter faces the water phase. Bolard (1986) concluded that the pore model fails to explain why the one-sided action is cation selective whereas the two-sided action is anion selective.

The amphotericin-cholesterol complex structure consisting of eight asymmetrical units was refined by the molecular mechanics technique (Khutorsky, 1992a). Figs. 2, 3, and 4 give the representations of the structural organization of the barrel. The half-pore is formed by six hydroxyl groups OH-2 · · · OH-7, one ester carbonyl group CO-8, and one methyl group CH_3-10 of each antibiotic molecule (Fig. 1). The pore diameter of the refined structure excludes the permeation of the nonelectrolytes of the size larger than glucose (Fig. 3). The external surface of the complex is formed by hydrophobic conjugated double-bond chains of the amphotericin and cholesterol molecules (Fig. 2 *b* and 3). The water-exposed part of the complex contains charged ammonium and carboxyl groups (Fig. 1). The stabilization of the complex is also caused by electrostatic interactions of ammonium and carboxyl groups of adjacent antibiotic molecules having 4.6-Å distances between C and N atoms. The same conclusion was made (Kasumov et al., 1979) based on the neutralization of one or both charges of the amphotericin B molecule by chemical modification or pH shift. Possibly some contribution to the stabilization of the complex could

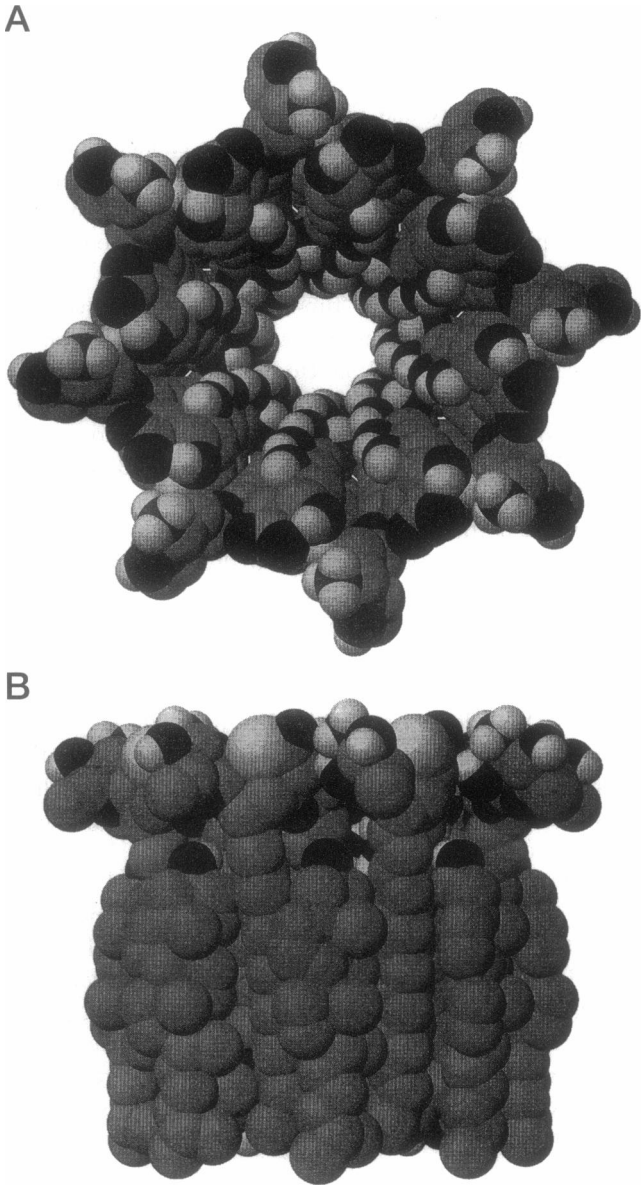

FIGURE 2 Overall views of the amphotericin-cholesterol complex. (*a*) View along the channel axis. (*b*) View in the perpendicular direction. Note that the complex is so closely packed that it is not easy to distinguish individual molecules. The next figure allows us to do this.

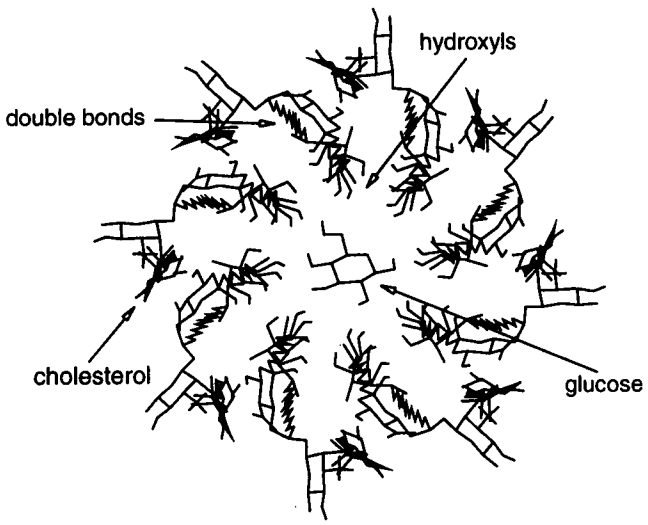

FIGURE 3 Skeletal view of the amphotericin-cholesterol complex along the channel axis. Carbohydrate hydrogens are omitted.

make the hydration water bridges connecting charged groups (Meddeb et al., 1992).

The shape of the pore is not regular, but contains narrow and wide areas. The pore is characterized by a wide polar entrance and a narrow area at the two oxygens O-6 and O-7 fitting the size of glucose (Fig. 3). The pore ligand groups are located in two areas. One of them containing OH-2 $\cdots$ OH-5 hydroxyls adjoins the water-exposed polar head end of the complex; another containing OH-6, OH-7, and CO-8 ligands adjoins the opposite nonpolar tail end of the complex. Let us refer to them as the wide and narrow ligand site, respectively. The short hydrophobic chains consisting of two methylene groups are located between them. The distances along the channel axis between the closest edge oxygens O-5 and O-6 of these two separated sites are about 4 Å. The intrasite distances between the neighboring oxygens are short enough to allow the formation of the hydrogen bonds (Khutorsky, 1992a). In reality the channel hydroxyl groups probably compete with the channel water molecules for hydrogen bonds.

The anionic conductance of two-sided channels is almost independent of the presence of monovalent cations. In contrast, in the absence of a permeant anion this channel is practically impermeable to cations. According to Borisova et al. (1986), the channel possesses intrinsic anion affinity, which is determined by the ligand OH dipoles oriented by positively charged protons toward the channel axis. These dipole orientations can produce a positive potential inside the pore, which favors anion binding and prevents a cation from entering the vacant channel. Anion binding compensates part of this potential and a cation can enter the channel. The formation of ion pairs in the channel is likely because the hydrophobic environment strongly enhances electrostatic interaction in it. Thus it was assumed that the channel can be vacant, with a bound anion, and with an ion pair. The authors suggested that the anion and cation can exchange places in the ion pair because monovalent inorganic ions have enough room to slip past each other in the 8-Å-diameter channel.

However, molecular mechanics studies (Khutorsky, 1992a) revealed that OH dipoles are oriented along the channel walls (Fig. 4). The hydroxyl hydrogens are approximately the same distance from the channel axis as the oxygens they are bonded to. This is because the adjacent C-O bonds are pointing toward the channel axis. According to the ab initio molecular orbital calculations performed for fragments of amphotericin B (Bolina-Marin et al., 1991), the absolute charge magnitudes of hydroxyl oxygens (~ -0.5) are nearly twice those of hydrogens (~ 0.3), which

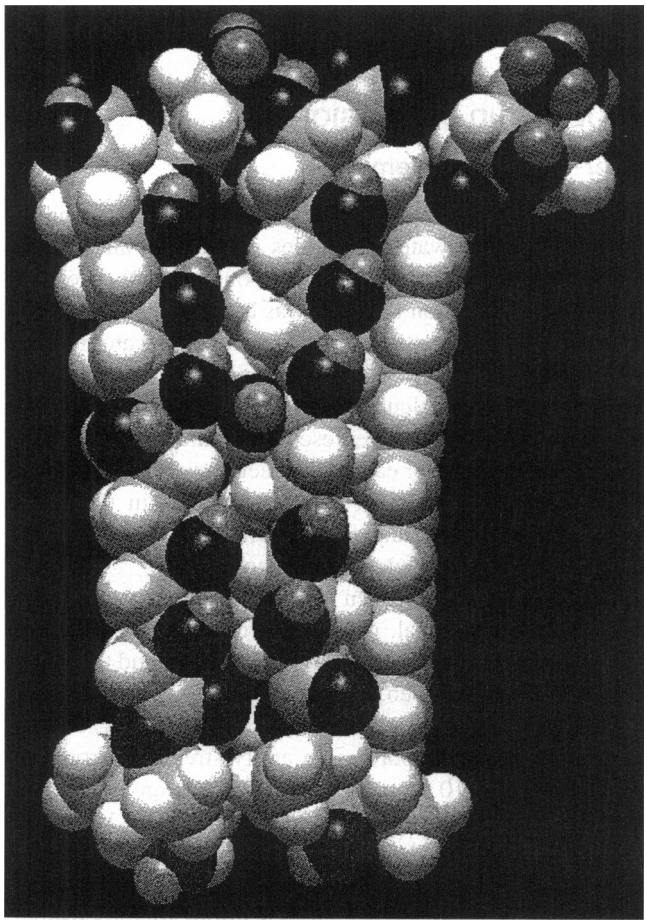

FIGURE 4 View from the channel axis to the channel wall. Two amphotericin and one incorporated cholesterol molecules are shown. The oxygen atoms of the ligand groups are black. It is clearly seen that the hydroxyl ligands form two separated sites. The intersite ligand distances are short enough for hydrogen binding.

at first glance implies that the pore has a cation rather than an anion affinity. In reality, with these charges the electrostatic energy potential calculated in a continuum medium approximation has the negative values inside the half-pore up to the tail end and positive values at the head entrance. The potential depends slightly on the number of antibiotic molecules included in the channel structure. It was proposed that the single-length channel works by attracting cations through the tail end. The double-length channel will be selective to anions because only the mouths are facing the solution. It is not clear how cations would overcome the electrostatic barrier at the head end of the half-pore. Apparently this model is inconsistent with the principle of microscopic reversibility.

To solve this problem comprehensively it is desirable to calculate the free energy profiles of individual ions and ion pairs in the channel-water systems. This could be done by "umbrella" sampling methods in which a biasing potential is used to localize the ion in a set of overlapping windows. However, at present these studies were completed only for the simplified models of gramicidin A in the absence of long-range interactions (Roux and Karplus, 1991; Elber et al., 1995). It seems that computational and methodological problems are much more complicated for the amphotericin B channel.

In this communication the author performed local molecular dynamics (MD) simulations starting from different positions of the ions in the water-filled channel that, nevertheless, made it possible to reveal some interesting details of the ions binding and to outline the possible reasons for the difference in the one- and two-sided channel selectivities. It was supposed that the open channel (with the above-described barrel structure) does not undergo overall rearrangements, such as a change in the number of molecules in the pore or essential mutual displacement of the molecules. Moreover, the transition of the channel from the open to the closed state, is probably not the result of such rearrangements, but may be caused by shrinking of the pore (Khutorsky, 1992a).

MATERIALS AND METHODS

MD simulations were carried out using the Insight and Discover package of BIOSYM Technology (San Diego, CA) on a Silicon Graphics workstation. The intramolecular and intermolecular energies were calculated by a CVFF force field of BIOSYM, which involves terms for stretching, bending, torsion, van der Waals, and electrostatic interactions. The partial charges of atoms for the electrostatic interactions were calculated by the PM3 method of the AMPAC/MOPAC module of BIOSYM for the whole molecule of amphotericin B. The relative magnitudes of the charges on the hydroxyl groups (~ -0.35 on oxygens and ~ 0.22 on hydrogens) are similar to those obtained by the ab initio calculations for fragments of the molecule (Bolina-Marin et al., 1991). The semiempirical charges are usually smaller in magnitude than the ab initio ones, but agree in sign and relative magnitude (Besler et al., 1990) and fit the CVFF force field.

The coordinates of the favorable structure of the amphotericin B-cholesterol complex consisting of eight antibiotic and eight cholesterol molecules (Khutorsky, 1992a) were used as the starting conformation for MD simulations. Because the simulation of the whole structure (containing 1699 atoms) is very computer intensive, only the atoms that have contacts with water and ions were considered. The cholesterol molecules and conjugated double-bond chains of the antibiotics were cut off. It is believed that the neglect of the hydrophobic exterior and environment can be an adequate approximation. There is a clear indication that the pore selectivity is due to the pore itself and independent of the sterols, surface membrane charge, and lipids (Kleinberg and Finkelstein, 1984). To avoid the distortion and scattering of the molecules of the complex, the edge bonds of the remaining structures (Fig. 1) were fixed in space. All other atoms were simulated without any positional constraints.

The "soak" command of Insight was used to generate the initial configuration of water molecules in the pore and in two adjacent entrance areas (Fig. 5). This procedure allows us to generate equilibrium water structures for systems of different topologies. At first the initial water configuration in the pore and the entrance parts of the pore was generated. Then, as in the paper of Leenders et al. (1994), the position-restrained outer water shells of 6 Å were generated to minimize the vacuum edge effects. A similar procedure (Roux et al., 1995) was applied to confine the bulk water caps at each mouth of the gramicidin channel. The simulated system consisted of 944 antibiotic atoms, 250 water molecules and ions simulated without any positional restrain, 32 fixed antibiotic atoms, and 246 position-restrained outer water molecules with a force constant of 100 kcal $mmol^{-1}$ $Å^{-2}$. About 26 water molecules were localized in the pore (see below), and others in the caps at the ends of the complex. No cutoff was chosen, so as to describe the long-range electrostatic interactions realistically. Thus all polar components of the channel were reproduced in the atomic detail. It is

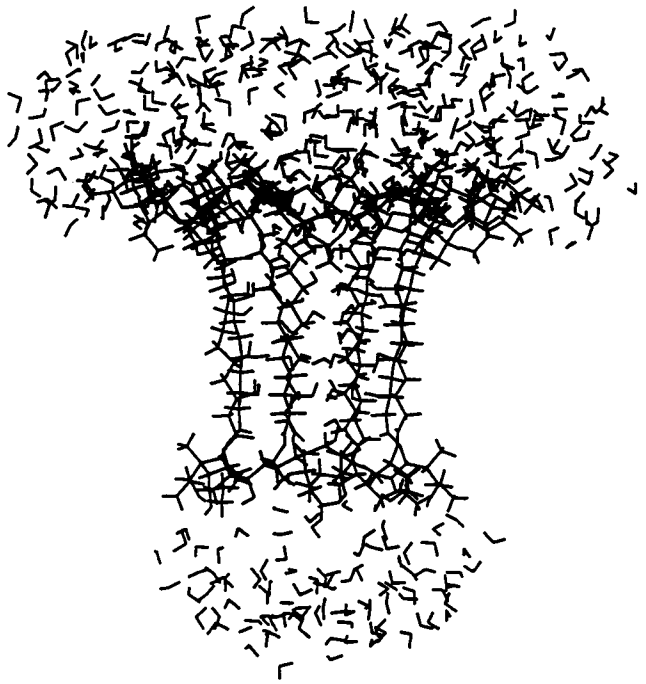

FIGURE 5 Overall view of the simulated channel-water system.

natural to assume that the ion coordination inside the pore is determined predominantly by the polar components. The MD simulation of Discover 2.9 was run at 300 K with an integration step of 1 fs. At first the water-filled channel was equilibrated within 50 ps until the total average potential energy remained constant (Fig. 6). One of the equilibrium configurations was chosen to generate ion-occupied systems. In accord with Borisova et al. (1986), the pore was considered singly or doubly occupied. For singly occupied channel the water molecules nearest to the centers of the narrow and wide ligand sites and at the head entrance of the pore were substituted by Cl^- or Na^+ and the systems were equilibrated for 50 ps. For doubly occupied channels two cases were considered. In one of them Cl^- and Na^+ were disposed in the same ligand site, in the second at different ligand sites. The equilibrium configurations of all systems were recorded every 0.02 ps during 200-ps equilibrium trajectories. The recorded configurations have been scanned by an additional program to obtain averaged structural parameters of the systems (see below).

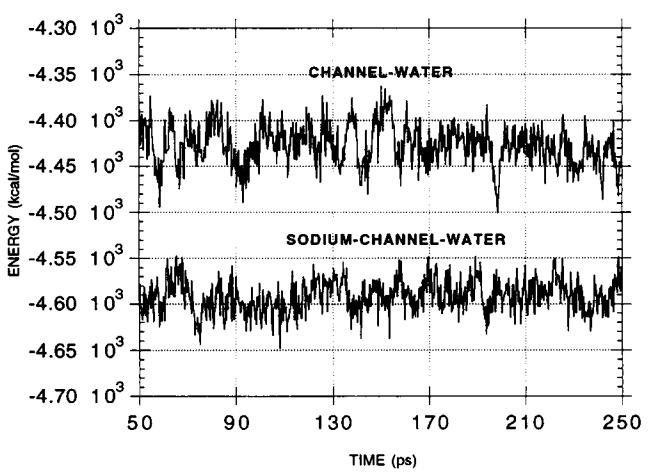

FIGURE 6 Total potential energies of the channel-water and ion-channel-water systems as functions of time for equilibrium configurations.

RESULTS AND DISCUSSION

Water-channel system

The water-channel trajectory has been scanned for the number and density of water molecules in the pore and water-channel and intrachannel hydrogen bonds. For the density distribution calculation the pore was considered as the cavity confined by the van der Waals spheres of the atoms. The cavity volumes for the different pore cross sections (with a length of 1 Å) were calculated as the accessible volumes for the probe water molecule represented by the van der Waals spheres. The density for each cross section was calculated as the ratio of the number of water molecules in the cross section to its volume and then normalized to the overall density of water molecules within the cavity.

The criteria for hydrogen bonds were taken as in the paper by Leenders et al. (1994): the distance between hydrogen and acceptor atoms was less than 2.5 Å and the angle between donor, hydrogen, and acceptor atoms has to exceed 135°.

Let us consider the pore as an entity stretching from the OH-2 to the CH_3-10 group (Fig. 1). The average number of water molecules located in the pore equals 25.6. Unlike the case of gramicidin A (see references in reviews of Jordan, 1987, and Khutorsky, 1992b), they do not create a single-file configuration, and some cross sections of the channel contain three or four water molecules (Fig. 7). The average number of water molecules per unit of channel length in the area extending from the OH-2 to the CO-8 group is 4.8

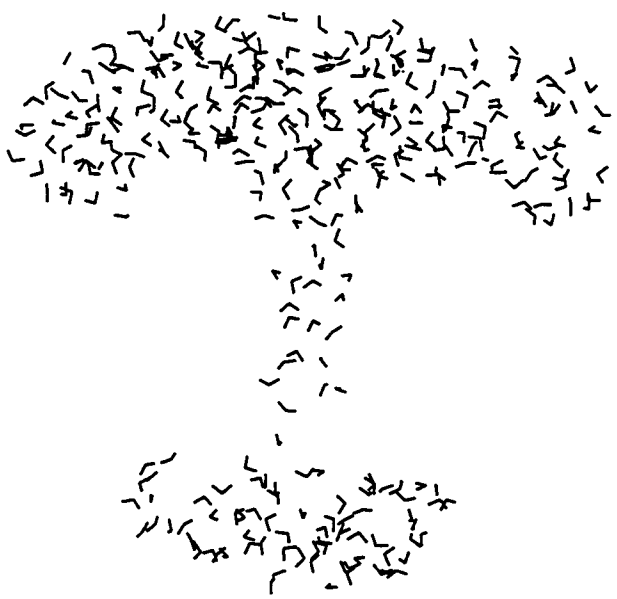

FIGURE 7 Snapshot of the equilibrium water configuration in the channel. The channel atoms are omitted. The sharp transition between the channel and cap water molecules can clearly be seen (see also Fig. 8).

times as large as that of the CO-8 · · · CH_3-10 area. The number and density of the water molecules essentially fall in the CH_3-10 area, which is clearly seen on the histograms (Fig. 8) and on the snapshot (Fig. 7). Thus there is a gap in the water density in the hydrophobic mouth of the half-pore or more extended gap in the center of the double-length pore. This waterless area would represent an essential Born energy barrier for the permeant ions in the later case. Certainly this statement should be verified by free energy calculations and experiments.

The probabilities that the ligand groups are involved with each other and with water molecules by hydrogen bonding are summarized in Table 1. The average numbers of the channel-water hydrogen bonds per equivalent ligand group range from 0.18 to 0.54. Thus each level of the equivalent ligand groups can be involved in two to four hydrogen bonds with channel water. The overall average number of the channel-water hydrogen bonds per ligand group of the channel is 0.32. Sixty-seven percent of the time of each water molecule is spent in ligand hydrogen bonding, ensuring its penetration into the channel.

The probabilities of ligand groups getting involved in hydrogen bonding with each other are remarkably higher (Table 1); the average numbers range from 0.32 to 1.48. The overall average number is 1.06. Some of the groups are involved in two, one, or no hydrogen bonds. The preferential intrachannel hydrogen bonds follow from the spatial structure of the complex, in which the ligand OH bonds are oriented along the channel walls.

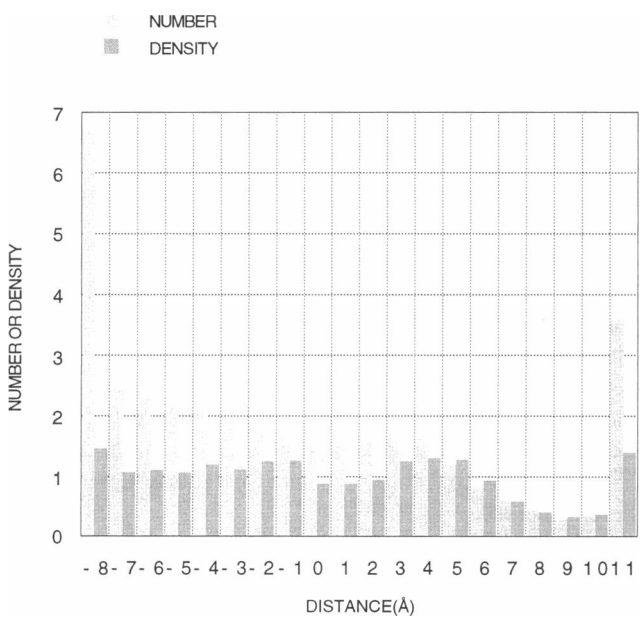

FIGURE 8 The water-oxygen number and normalized density linear distribution histograms along the half-pore long axis. The edge bars of the histograms belong to the water caps attached to the channel. The gap in the water density is clearly seen at the nonpolar right end of the pore. There also is a slight reduction in the number and density of the water molecules at the central intersite hydrophobic area of the pore.

TABLE 1 The average numbers of hydrogen bonds in the channel-water system

	OH-2	OH-3	OH-4	OH-5	OH-6	OH-7	CO-8
LL	1.00	1.44	1.44	0.88	1.12	1.16	0.32
LW	0.24	0.32	0.18	0.22	0.42	0.54	0.30

LL is the average number of hydrogen bonds between a chosen ligand group and others. LW is the average number of hydrogen bonds between a chosen ligand group and water molecules.

Strong correlation between orientations of hydroxyls groups was observed. The pair bond orientation correlation functions (defined in Table 2) revealed the preferential parallel intrasite OH bond orientations. Weak intersite correlation showed only the closest OH-5 and OH-6 groups (Table 2). Hydroxyl groups belonging to wide or narrow sites of the pore were dominantly oriented in parallel to each other and the pore axis. At these orientations the distances between the axis and oxygen and hydrogen of the same group differed rather slightly (Table 3). Dominant oxygen charges would cause considerable negative electrostatic potential to be concentrated in the pore (see below). The distances are close to those obtained by the molecular mechanics technique for the complex containing uncut antibiotic and cholesterol molecules (Khutorsky, 1992a). Obviously the shape of the pore is defined by the packing of the hydrophilic chains of the lactone ring that justifies the truncated structure, brought about by the complication of the channel.

Anion coordination in the channel

Simulations showed that chloride can be coordinated both in the wide and the narrow ligand sites of the half-pore. This implies that there is an area of unfavorable energy located between them. Actually, the electrostatic term of the anion-channel interaction energy has a high value inside the half-pore (Fig. 9) that is naturally determined by negatively charged ligand oxygens, whose electrostatic field dominates the field of the hydrogens. This finding is in accord with the anion two energy barrier profile (Borisova et al., 1986), which was used for the interpretations of experimental data for the double-length channel. The final conclusion about the shape of the profile would be made on the basis of umbrella sampling simulations.

TABLE 2 Pair bond orientation correlation functions $\langle e_i\, e_j \rangle$

$i \backslash j$	3	4	5	6	7
2	0.71	0.61	0.50	0.01	0.00
3	1.00	0.75	0.63	0.02	0.01
4		1.00	0.67	0.05	0.04
5			1.00	0.12	0.07
6				1.00	0.85

e_i and e_j ($j > i$) are the unit vectors directed along the projections of the $(OH)_i$ and $(OH)_j$ bonds (Fig. 1) on the channel axis.

TABLE 3 Average distances (Å) of ligand oxygens and hydrogens from the channel axis

Number*	Oxygen	Hydrogen
2	7.6	7.7
3	6.8	7.0
4	5.9	5.8
5	6.9	6.1
6	5.1	4.8
7	5.0	4.5
8	5.7	

*See in Fig. 1 the numbers of the ligand groups.

TABLE 4 Coordination parameters of ions and ion pairs in the channel

Anion				Cation					
T	W	L_1	L_2	T	W	L_1	L_2	d	P
Cl^-; narrow site									
5.97	4.57	1.01 (6)	0.39 (7)						
Cl^-; wide site									
5.58	4.22	0.86 (3)	0.50 (4)						
Na^+; narrow site									
				5.63	3.32	1.10 (6)	1.21 (7)		
Contact pair; narrow site				Narrow site					
3.45	2.80	0.45 (6)		3.80	2.00	1.00 (7)	0.80 (8)	2.71	1.00
Shared pair; narrow site				Wide entrance					
5.13	4.13	1.00 (7)		5.87	5.87			5.70	0.83
Shared pair; wide site				Narrow site					
5.80	4.55	0.60 (4)	0.65 (5)	5.20	4.60	0.60 (6)		4.91	0.95

T, W, L_1, and L_2 are total, water, and ligand coordination numbers for the anion and cation, respectively. The numeration of coordinated ions ligand groups is indicated in parentheses.
d is the average distance (Å) between ions in an ion pair.
P is the probability of ion pair formation.

Let us consider first the anion coordination in the narrow ligand site of the channel. The criterion for a ligand group or water molecule to belong to an ion coordination sphere was that the distance between an ion and an oppositely charged atom of the ligand or water would not exceed 2.8 Å.

The total coordination number of the anion is 5.97 (Table 4). It is localized in the vicinity of OH-6 and OH-7 hydrogens, whose contribution to the coordination number is 1.40. The dominant part of this value (1.01) comes from the OH-6 ligand. There are 4.57 water molecules localized in the chloride coordination sphere. Three motifs of ion coordination were monitored (Fig. 10). The dominant one occurs when the anion is bound to one OH-6 or one OH-7 ligand; the probability of the motif is 0.67. The 0.29 part of the simulated time the ion spends bound to the OH-6 and OH-7 ligand groups, and the rest of the 0.05 trajectory time to two OH-6 and one OH-7 ligand group. The anion stabilization in the vicinity of the hydrogens of these groups can be accounted for by repulsion from the central part of the complex due to the negative electrostatic potential inside the pore (Fig. 9) and from the narrow entrance of the pore due to the presence of CO-8 oxygens and a gap in the water density.

In the wide ligand site of the complex, the anion is localized in the vicinity of the OH-3 and OH-4 ligand groups. The total coordination number is close to the first case but more evenly distributed between ligand groups. As in the first case, the binding with water is dominant.

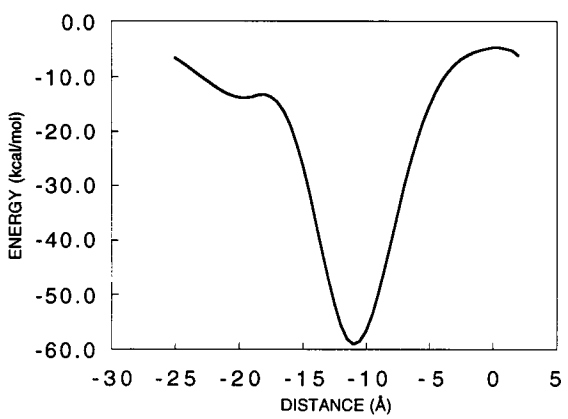

FIGURE 9 The electrostatic term of the cation-complex interaction energy along the axis of the fixed double-length channel. Only the half of the curve is shown because it is symmetrical relative to the origin located at the double-length channel geometrical center.

The coordination of the anion by the ligand groups in the polar entrance region of the channel was not observed, but in some configurations two water molecules out of six from the ion coordination sphere were hydrogen bonded to the OH-2 ligand (Fig. 11). This solvent-shared complex could be considered as a preliminary step in the anion binding with the channel walls in the wide ligand site of the pore. Apparently there is a translocation barrier to the anion entering the pore due to the replacement of two water molecules by two ligand groups in the anion coordination sphere.

It is necessary to note that in both bound states the anion is essentially displaced from the channel axis (see anion trajectories in Fig. 12) and bound to the channel walls, where it is hydrated by more than four water molecules. Because the diameter of the amphotericin channel is twice that of the gramicidin channel, this displacement is expressed more than in gramicidin A (see Jordan, 1987, or Khutorsky, 1992b). Thus permeant ions should deviate from the channel axis.

Cation coordination in the channel

The simulations showed that Na^+ drifts toward the narrow ligand site of the pore (Fig. 13 and 14). The strong affinity of the cation to this area is accounted for by the electrostatic terms of the ion-channel interaction energy having the deep minimum inside the half-pore. The binding of the cation in

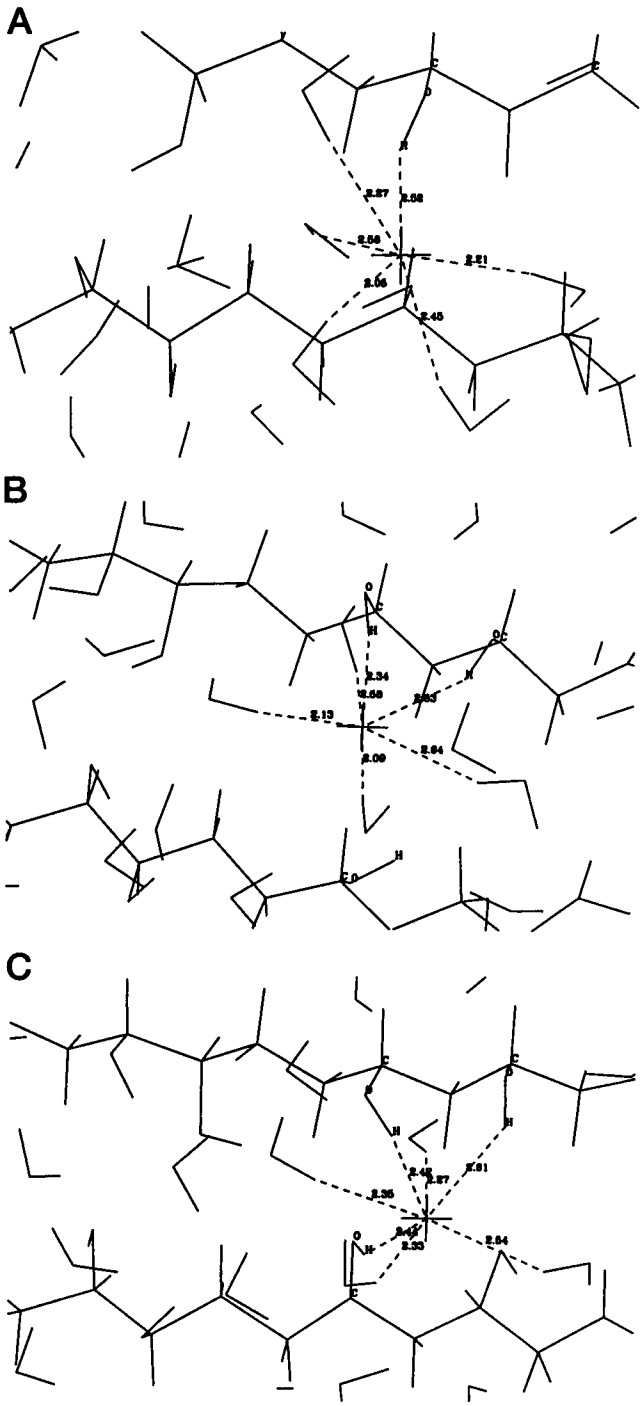

FIGURE 10 Three motifs of the anion coordination in the nonpolar part of the channel. (*a*, *b*, and *c*) The anion coordinated by one, two, and three ligand groups, respectively. The ion is represented by crosses. The ligands are OH-6 and OH-7.

the wide ligand site is unfavorable relative to this term (Fig. 9).

The coordination number of the cation is 5.63 (Table 4). The ligand contribution of 2.31 to the coordination number is noticeably higher than in the case of the anion. Consequently the water-ion coordination number (3.32) is smaller.

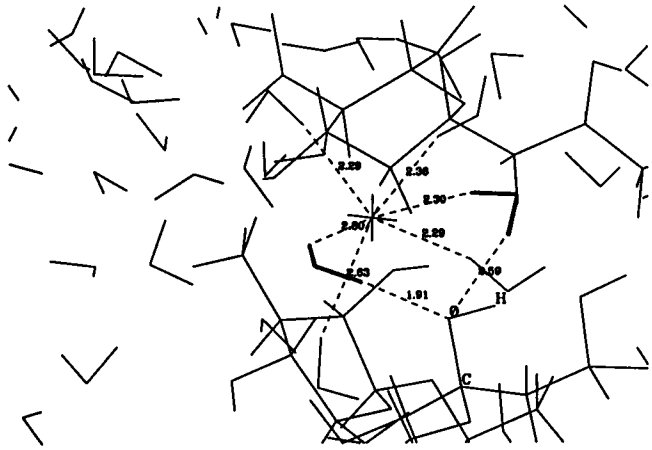

FIGURE 11 Snapshot of the solvent-shared complex at the entrance part of the pore. The hydrated anion is located in the vicinity of the OH-2 ligand. Two shared water molecules are represented by thick lines.

As in the case of the anion, there are three motifs of the cation coordination (Fig. 13). The favorable one occurs when the cation is bound to two nonequivalent ligand oxygens O-6 and O-7. In the less favorable case, the cation is bound to one O-6 and two O-7 oxygens or two O-6 and one O-7 oxygen. On rather rare occasions, the cation is bound to

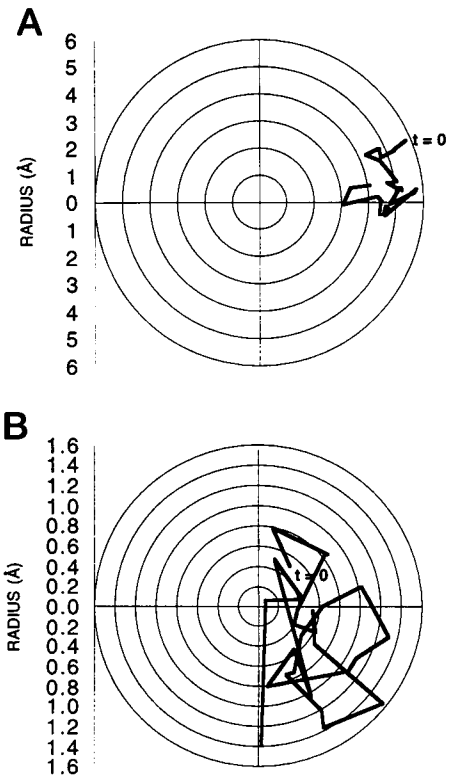

FIGURE 12 Chloride motions in the planes perpendicular to the channel axis. (*a* and *b*) The wide and narrow ligand sites, respectively. The time intervals between points are 10 ps. Note that the ion trajectories strongly deviate from the channel axis.

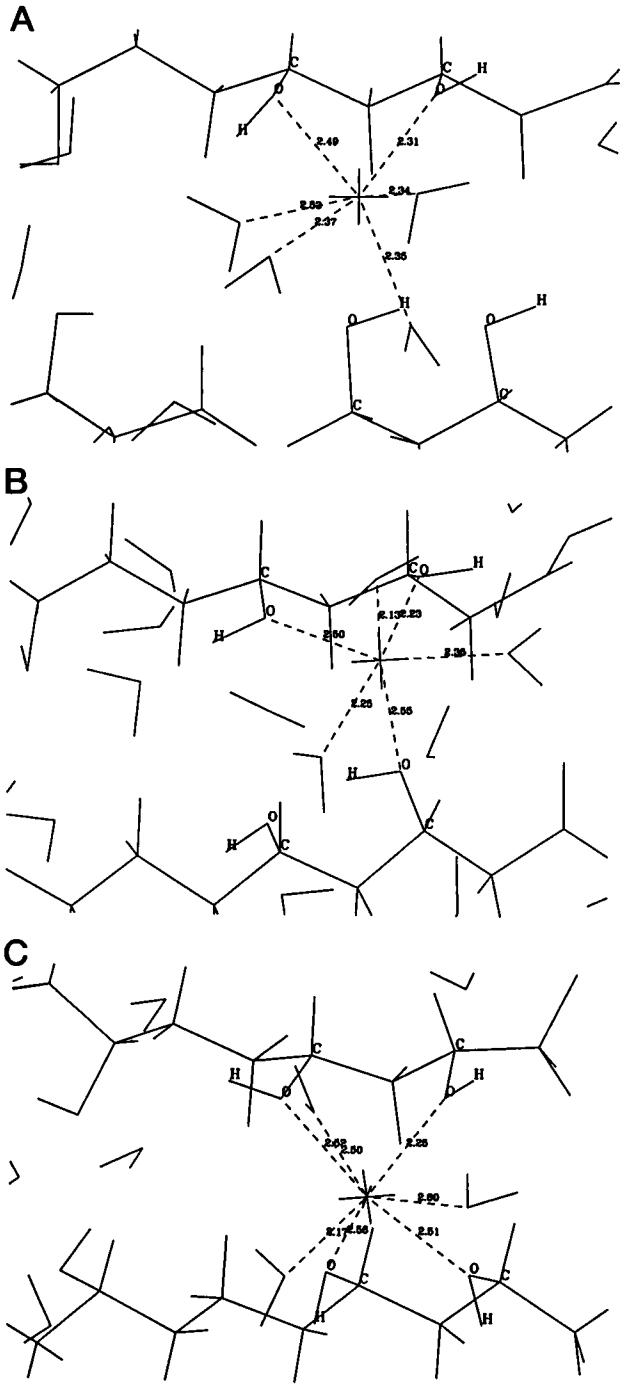

FIGURE 13 Three motifs of the cation coordination in the channel. (*a*, *b*, and *c*) The cation coordinated by two, three, and four ligand groups, respectively. The ligands are OH-6 and OH-7.

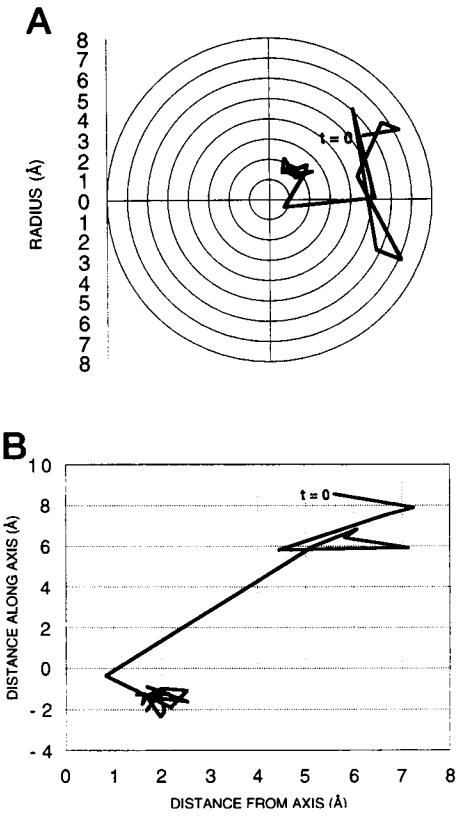

FIGURE 14 The sodium ion motion in the planes perpendicular to (*a*) and along (*b*) the channel axis. The channel axis is directed from the narrow to the wide site with the origin in the geometrical center of the channel. Note that the ion drifts from the wide to the narrow site of the channel.

two O-6 and two O-7 oxygens. The relative probabilities of these motifs are 0.78, 0.17, and 0.06, respectively.

Thus both the cation and anion have strong binding sites in the pore. The results thus obtained could easily explain the cation permeability of the half-pore. No doubt this explanation needs further support and verification by means of simulation and experimental techniques. Let us admit that the electrostatic term of the ion-channel interaction dominates in the ion free energy profile formation. This implies that the half-pore may have an energy well for cations and a barrier for anions. The double length channel may consistently have two wells and a barrier between them for cations and two barriers and a low-energy area between them for anions. Unlike the double-length channel, the single-length channel is permeable to cations because its nonpolar end is facing the water phase. Apparently the free energy barrier of anions passing through the waterless central part of the two-sided pore could be somewhat lower relative to cations. Actually, anions would overcome only the Born energy barrier, whereas cations would overcome both electrostatic and Born energy barriers. Thus the central waterless part of the double-length pore may serve as a selective anion/cation filter. The question of how cations can pass through the filter will be discussed below.

Anion-cation pair coordination

The motif of the contact ion pair coordination is shown in Fig. 15. The average distance between ions is 2.71 Å. The cation is localized more closely to the nonpolar end than the anion and is bound to O-7 and O-8 ligand oxygens. The anion is localized in the vicinity of O-6 oxygens. Attempts

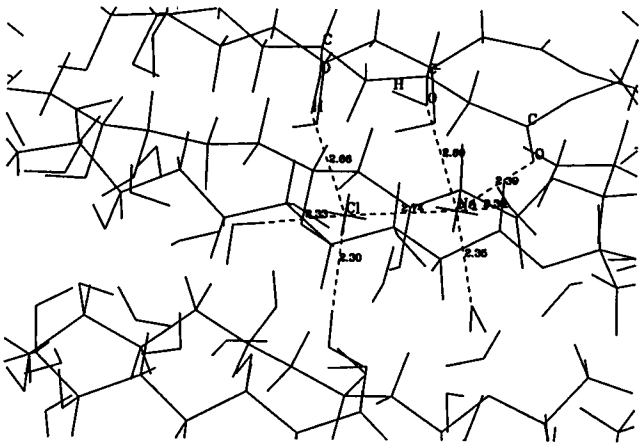

FIGURE 15 Snapshot of the contact ion pair coordination in the half-pore. The cation is shifted toward the tail end of the pore. The anion ligand is OH-6, and the cation ligands are OH-7 and CO-8.

made to reverse the orientation of the ions were unsuccessful (see trajectories in Fig. 16). This result naturally follows from the repulsion of the anion from CO-8 oxygens and indicates that the ions can slip past each other (Borisova et al., 1986) in the narrow central part of the double-length channel.

The coordination numbers of the ions in the pair relative to the water molecules and ligand groups are much lower than for individual ions (Table 4). In the case of the cation the coordination number is 3.80. The ligand groups and water molecules contribute evenly to the coordination number: 1.80 and 2.00, respectively. O-8 has a somewhat lower probability to be bound to a cation than O-7. In the case of the anion, the contribution of 2.80 by water molecules to the coordination number (3.45) is dominant.

The question raised earlier of how the cation could cross the filter area can now be reasonably answered: the crossing is much easier for an electro-neutral ion pair. In this model the anion serves as a shuttle, migrating between two ion-binding sites in the central part of the double-length channel.

The simulation showed that there exists a solvent-shared stable state of the cation and the anion, in which the anion was localized in the narrow site and the cation in the wide polar entrance of the half-pore (Fig. 17 and 18). The average distance between ions was 5.70 Å, twice as large as that of the contact ion pair (Table 4). For eighty-three percent of the simulation time the ions were in the solvent-shared states, in which one water molecule belonged to both the anion and the cation coordination spheres. The anion was localized in the vicinity of the OH-7 ligand group, whose contribution to the coordination number was about 1/5. The cation coordination sphere consisted only of water molecules.

The stability of the solvent-shared state is defined by the water molecule oriented along the electrostatic field of both ions (Fig. 17). This state can be considered as the intermediate stable state for the cation entering the channel and final one for the cation leaving the channel.

The similar solvent-shared state (which occupied 95% of the simulation time) was also seen in the position-reversed

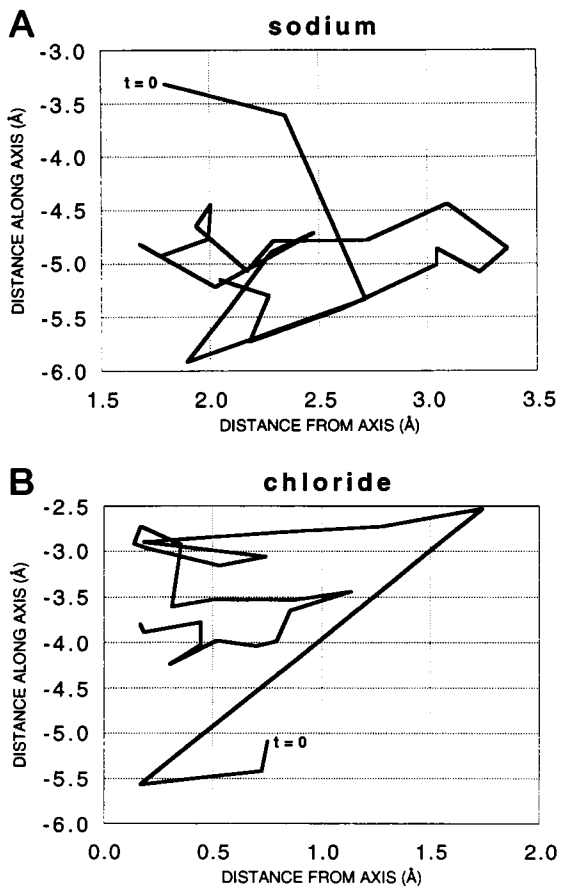

FIGURE 16 Ion motions in the contact ion pair. (*a*) Sodium ion. (*b*) Chloride. Note that ions exchange positions during motions.

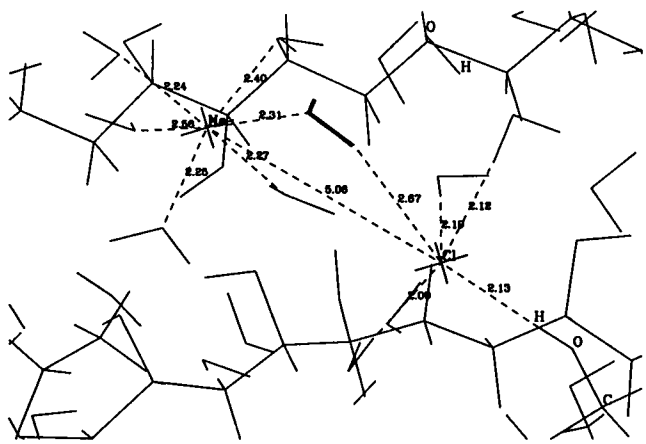

FIGURE 17 Snapshot of the solvent-shared ion pair coordination in the monomer channel. The cation is located in the wide entrance of the pore. The ligand for anion is OH-7. One shared water molecule is represented by thick lines.

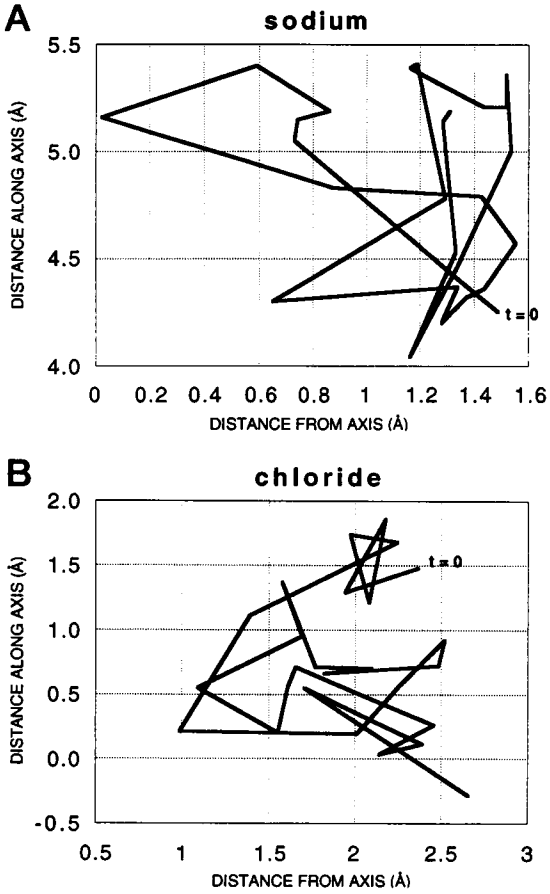

FIGURE 18 Ion motions in the solvent-shared pair. (*a*) Sodium ion. (*b*) Chloride.

ion pair. In this state the anion is mainly localized in the vicinity of OH-6 and the cation in the vicinity of OH-4 and OH-5 ligand groups, respectively (Table 4). This state can be considered as intermediate for the anion entering the cation-occupied channel.

CONCLUSION

The ion-water-amphotericin B channel MD simulation presented here revealed some fine features of the transport mechanisms. It is necessary to note that the comprehensive model of the channel permeability and selectivity can be constructed only on the basis of ion free energy profile calculations for the channels with proven structures. Given the complexity of the problem, the obtained results are acceptable as a way to start constructing a comprehensive microscopic understanding.

The average number of water molecules located in the half-pore is 25.6. Unlike the case of gramicidin A, they do not create a single-file configuration, and in some cross sections of the channel there are three or four water molecules. There is a reduction in the water density in the nonpolar mouth of the half-pore (Fig. 5) or in the central part of the two-sided pore. This waterless area should create an essential Born energy barrier for the permeant ions. Each level of the equivalent ligand groups connects the two to four hydrogen bonds with water molecules localized in the channel. A water molecule spends 67% of its lifetime in the pore involved in hydrogen bonding with ligand groups that should facilitate water penetration into the channel. The probabilities that ligand groups are involved with each other by hydrogen bonding are noticeably higher (Table 1). The overall average number of hydrogen bonds per one group is about one, but some of the groups are involved in two, one or no hydrogen bonds. Hydroxyl groups belonging to the same site of the pore tend to be oriented in parallel to each other and to the pore axis. The preferential intrachannel hydrogen binding follows from the spatial structure of the complex, in which the ligands adjacent to C-O bonds are pointing toward the channel axis (Khutorsky, 1992a).

Both anion and cation have strong binding sites in the channel

The anion has two binding sites in the half-pore, located in its opposite parts. Apparently this is determined by the high value of the electrostatic term of the anion-channel interaction energy inside the half-pore (Fig. 9). The coordination number of the anion is about 6. Binding with water is dominant; more than four water molecules are localized in the anion coordination sphere (Table 4). Three motifs of ion coordination were monitored. The dominant motif occurred when the anion was bound with one ligand group. The rest of the simulated time the ion was bound to two or three ligand groups (Fig. 10).

The strong affinity of the cation to the pore is accounted for by the negative electrostatic potential in the channel (Fig. 9). The coordination number of the cation is 5.63. The ligand contribution to the coordination number of 2.31 is noticeably higher than in the case of the anion (Table 4). As in the case of the anion, there are three motifs of cation coordination (Fig. 13). The favorable one occurs when the cation is bound to two nonequivalent ligand oxygens. In the less favorable case, the cation is bound to three oxygens. On rather rare occasions the cation is bound to four oxygens.

It is necessary to note that the anion and cation are essentially displaced from the channel axis and bound to the channel walls (see ion trajectories in Figs. 12, 14, 16, and 18). Thus permeant ions should deviate from the channel axis.

The simulations could explain the cation permeability of the half-pore. Unlike the two-sided channel, the one-sided channel is permeable to cations because its nonpolar end is facing the water phase. Apparently the free energy barrier of anions passing through the waterless central part of the double-length pore could be somewhat lower relative to cations. Actually, anions should overcome only the Born energy barrier, whereas cations should overcome both electrostatic and Born energy barriers.

In the contact ion pair the cation is located closer to the narrow tail end than the anion and is bound by two ligand

oxygens (Fig. 15). The attempts to reverse the ion orientation were unsuccessful. This indicates that the ions can slip past each other in the narrow central part of the double-length channel. The electro-neutral ion pair can more easily overcome the waterless central channel area than the individual cation. The anion probably serves as a shuttle, migrating between two ion-binding sites in the central part of this channel.

There exist so-called solvent-shared ion pair states, in which the ions are located in the opposite ends of the half-pore (Fig. 17). The average distance between ions is twice as large as that of the contact ion pair (Table 4). The stability of the solvent-shared state is defined by the water molecule oriented along the electrostatic field of both ions. These states can be considered as the intermediate stable state in the process of ion pair formation.

I thank Dr. Peter C. Jordan and Dr. David Gill for their helpful comments on the manuscript.

REFERENCES

Andreoli, T. E. 1973. On the anatomy of amphotericin B-cholesterol pores in lipid bilayer membranes. *Kidney Int.* 4:337–345.

Benz, R., O. Frohlich, R. Lauger, and M. Montal. 1975. Electrical capacity of black lipid films and lipid bilayers made from monolayers. *Biochim. Biophys. Acta.* 394:323–334.

Besler, B. E., K. M. Merz, Jr., and P. A. Kollman. 1990. Atomic charges derived from semiempirical methods. *J. Comput. Chem.* 11:431–439.

Bolard, J. 1986. How do the polyene macrolide antibiotics affect the cellular membrane properties? *Biochim. Biophys. Acta.* 864:257–304.

Bolard, J., P. Legrand, F. Heitz, and B. Cybulska. 1991. One-sided action of amphotericin B on cholesterol-containing membranes is determined by its self-association in the medium. *Biochemistry.* 30:5707–5715.

Bolina-Marin, M., M. Moreno-Bello, and I. Ortega-Blake. 1991. A microscopic electrostatic model for the amphotericin B channel. *Biochim. Biophys. Acta.* 1061:65–77.

Borisova, M. P., R. A. Brutyan, and L. N. Ermishkin. 1986. Mechanism of anion-cation selectivity of amphotericin B channels. *J. Membr. Biol.* 90:13–20.

Brajtburg, J., W. J. Powderly, G. S. Kobayashi, and G. Medoff. 1990. Amphotericin B: current understanding of mechanisms of action. *Antimicrob. Agents Chemother.* 34:183–188.

Cass, A., A. Finkelstein, and V. Krespi. 1970. The ion permeability induced in thin lipid membranes by the polyene antibiotics nystatin and amphotericin B. *J. Gen. Physiol.* 56:100–124.

Cohen, E. B. 1986. Concentration- and time-dependence of amphotericin B induced permeability changes across ergosterol-containing liposomes. *Biochim. Biophys. Acta.* 857:117–122.

De Kruijff, B., and R. A. Demel. 1974. Polyene antibiotics-sterol interactions in membranes of *Acoleplasma laidlawii* cell and lecithin liposomes. III. Molecular structure of the polyene antibiotic-cholesterol complexes. *Biochim. Biophys. Acta.* 339:57–70.

De Kruijff, B., W. J. Gerristsen, W. J. Oerlemans, R. A. Demel, and L. L. M. Van Deenen. 1974. Polyene antibiotics-sterol interactions in membranes of *Acoleplasma laidlawii* cell and lecithin liposomes. I. Specificity of the membrane permeability changes induced by the polyene antibiotics. *Biochim. Biophys. Acta.* 339:30–43.

Elber, R., D. P. Chen, D. Rojewska, and R. Eisenberg. 1995. Sodium in gramicidin: an example of permion. *Biophys. J.* 68:906–924.

Ermishkin, L. N., Kh. M. Kasumov, and V. M. Potseluyev. 1976. Single ionic channels induced in lipid bilayers by polyene antibiotics amphotericin B and nystatin. *Nature.* 262:698–699.

Ermishkin, L. N., Kh. M. Kasumov, and V. M. Potseluyev. 1977. Properties of amphotericin B channels in a lipid bilayer. *Biochim. Biophys. Acta.* 470:357–367.

Finkelstein, A., and R. Holz. 1973. Aqueous pores created in thin lipid membranes by the polyene antibiotics nystatin and amphotericin B. *In* Membranes. Lipid Bilayers and Antibiotics, Vol. 2. G. Eisenman, editor. Marcel Dekker, New York. 377–408.

Gallis, H. A., R. H. Drew, and W. W. Pickard. 1990. Amphotericin B: 30 years of clinical experience. *Rev. Infect. Dis.* 12:308–329.

Gruda, I., P. Nadeau, J. Brajtburg, and G. Medoff. 1980. Application of different spectra in the UV-visible region to study the formation of amphotericin B complexes. *Biochim. Biophys. Acta.* 602:260–268.

Herve, M., J. C. Dubouzy, E. Borowski, B. Cybulska, and C. M. Gary-Bobo. 1989. The role of the carboxyl and amino groups of polyene macrolides in their interactions with sterols and their selective toxicity. A ^{31}P-NMR study. *Biochim. Biophys. Acta.* 980:261–272.

Jordan, P. C. 1987. Microscopic approaches to ion transport through transmembrane channels. The model system gramicidin. *J. Phys. Chem.* 91:6582–6591.

Kasumov, Kh. M., M. P. Borisova, L. M. Ermishkin, V. M. Potseluyev, A. Ya. Silberstein, and V. A. Vainshtein. 1979. How do ionic channel properties depend on the structure of polyene antibiotic molecules? *Biochim. Biophys. Acta.* 51:229–237.

Khutorsky, V. E. 1992a. Structures of amphotericin B-cholesterol complex. *Biochim. Biophys. Acta.* 1108:123–127.

Khutorsky, V. E. 1992b. Structure-activity relationships of ion transport compounds. *Int. J. Quantum Chem. Quantum Biol. Symp.* 19:187–196.

Kleinberg, M. E., and A. Finkelstein. 1984. Single-length and double-length channels formed by nystatin in lipid bilayer membranes. *J. Membr. Biol.* 80:257–269.

Leenders, R., W. F. van Gunsteren, H. J. C. Berendsen, and A. J. W. G. Visser. 1994. Molecular dynamics simulations of oxidized and reduced *Clostridium beijerinckii* flavodoxin. *Biophys. J.* 66:634–645.

Marty, A., and A. Finkelstein. 1975. Pore formed in lipid bilayer membranes by nystatin. Differences in its one-sided and two-sided action. *J. Gen. Physiol.* 65:515–526.

Meddeb, S., J. Berges, J. Caillet, and J. Langlet. 1992. Comparative theoretical study of the conformations of amphotericin methyl ester and amphotericin polar heads in the presence of water. *Biochim. Biophys. Acta.* 1112:266–272.

Roux, B., and M. Karplus. 1991. Ion transport in a gramicidin-like channel: structure and thermodynamics. *Biophys. J.* 59:961–981.

Roux, B., B. Prod'hom, and M. Karplus. 1995. Ion transport in the gramicidin channel: molecular dynamics study of single and double occupancy. *Biophys. J.* 68:876–892.

Van Hoogevest, P., and B. De Kruijff. 1978. Effect of amphotericin B on cholesterol-containing liposomes of egg phosphatidylcholine and didocosenoyl phosphatidylcholine. A refinement of the model for the formation of pores by amphotericin B in membranes. *Biochim. Biophys. Acta.* 511:397–407.

Vertut-Croquin, A., J. Bolard, M. Chabert, and G. Gary-Bobo. 1983. Differences in the interaction of the polyene antibiotic amphotericin B with cholesterol- or ergosterol-containing phospholipid vesicles. A circular dichroism and permeability study. *Biochemistry.* 22:2939–2944.